

# Spatial variations in sedimentary N-transformation rates in the North Sea (German Bight)

Alexander Bratek<sup>1,2</sup>, Justus E.E. van Beusekom<sup>1,3</sup>, Andreas Neumann<sup>1</sup>, Tina Sanders<sup>1</sup>, Jana Friedrich<sup>1</sup>, Kay-Christian Emeis<sup>1,2</sup> and Kirstin Dähnke\*<sup>1</sup>

<sup>1</sup> Helmholtz-Zentrum Geesthacht, Institute for Coastal Research, Geesthacht, Germany

<sup>2</sup> University of Hamburg, Center for Earth System Research and Sustainability, Institute for Geology, Hamburg, Germany

<sup>3</sup> University of Hamburg, Center for Earth System Research and Sustainability, Institute for Hydrobiology and Fisheries, Hamburg, Germany

\* Correspondence to: [kirstin.daehnke@hzg.de](mailto:kirstin.daehnke@hzg.de)

## Abstract

In this study, we investigate the role of sedimentary N cycling in the Southern North Sea. We present a budget of ammonification, nitrification and sedimentary  $\text{NO}_3^-$  consumption / denitrification in contrasting sediment types of the German Bight (Southern North Sea), including novel net ammonification rates. We incubated sediment cores from four representative locations in the German Bight (permeable, semi-permeable and impermeable sediments) with labeled nitrate and ammonium to calculate benthic fluxes of nitrate and ammonium and gross rates of ammonification and nitrification. Ammonium fluxes generally suggest oxic degradation of organic matter, but elevated fluxes at one sampling site point towards the importance of bio-irrigation or short-term accumulation of organic matter. Sedimentary fluxes of dissolved inorganic nitrogen are an important source for primary producers in the water column, supporting ~7 to 59 % of the average annual primary production, depending on water depth.

We find that ammonification and oxygen penetration depth are the main drivers of sedimentary nitrification, but this nitrification is closely linked to denitrification. One third of freshly produced nitrate in impermeable sediment and two-thirds in permeable sediment were reduced to  $\text{N}_2$ . The semi-permeable and permeable sediments are responsible for ~68 % of the total benthic  $\text{N}_2$  production rates, which, based solely on our data, amounts to ~1030 t  $\text{N d}^{-1}$  in the southern North Sea. Thus, we conclude that semi-permeable and permeable sediments are the main sinks of reactive N, counteracting eutrophication in the southern North Sea (German Bight).

## 30 **1 Introduction**

31 The continental shelves and coastal margins make up for <9 % of the total area of ocean surface, but are responsible  
32 for vast majority of the biogeochemical cycling both in the water column and in the sediments (Jorgensen, 1983).  
33 For instance, 30 % of global marine primary production occurs in coastal, estuarine and shelf systems (LOICZ,  
34 1995), and nutrient regulation in shelf sediments is a particularly valuable ecosystem service (Costanza et al.,  
35 1997).

36 The German Bight is part of the southern North Sea and is bordered by densely populated and industrialized  
37 countries, and receives large amounts of nutrients via river discharge (e.g., Rhine, Maas, Elbe, Weser, Ems) (Los  
38 et al., 2014). This caused clear eutrophication symptoms such as phytoplankton blooms, oxygen deficiencies and  
39 macrobenthos kills especially during the 1980s (Hickel et al., 1993; von Westernhagen et al., 1986) in the North  
40 Sea. In the adjacent Wadden Sea intense phytoplankton blooms, a possible decrease of seagrass and massive  
41 blooms of opportunistic macroalgae were attributed to eutrophication (e.g. Cadée and Hegemann, 2002). Since the  
42 mid 1980s, the nitrogen (N) loads into the German Bight have been decreasing, but the entire SE North Sea is still  
43 flagged as an eutrophication problem area (OSPAR, 2010).

44 Nitrogen availability increases primary production on a variety of spatial and temporal scales. At present, major  
45 nitrogen sources for the Southern North Sea are agricultural and urban waste water, and to a lesser extent, a variety  
46 of reactive N emission (e.g., nitrogen oxides from burning fossil) (Emeis et al., 2015).

47 Internal N cycling in sediments (e.g., assimilation, ammonification and nitrification) change the distribution and  
48 speciation of fixed N, but not the overall amount of N available for primary production (Casciotti, 2016). Reduction  
49 of reactive nitrogen through denitrification and anammox in anoxic conditions back to unreactive N<sub>2</sub>, however,  
50 does remove N from the biogeochemical cycle (Neumann et al., 2017).

51 Because these eliminating processes are confined to suboxic and anoxic conditions, they only occur in sediments  
52 in the generally oxygenated North Sea. Due to its putative relevance as an ecosystem service, denitrification has  
53 been subject to many studies, but ammonification as a source of N to primary production so far received much less  
54 attention. This is in part due to the complexity created by coupled ammonification-nitrification in which different  
55 N processes, such as assimilation and denitrification, interact and affect the NH<sub>4</sub><sup>+</sup> and NO<sub>3</sub><sup>-</sup> concentrations in pore  
56 waters. To our knowledge, no ammonification rates in the North Sea have been quantified, whereas nitrification  
57 rates in permeable sediments were found to be in the same order of magnitude as denitrification rates (<0.1 to ~3.0  
58 mmol m<sup>-2</sup> d<sup>-1</sup>, Tab. 1) (Marchant et al., 2016). N loss in the German Bight has been studied by several authors (e.g.  
59 Deek et al., 2013) showing high spatial, temporal and seasonal variability.

60 The main N loss process in the North Sea is denitrification, whereas and anammox plays a minor role (Bale et al.,  
61 2014; Marchant et al., 2016). The main drivers of denitrification are organic matter content and permeability of  
62 the sediment (Neumann, 2012), and recent studies suggest that permeable sediments account for about 90  
63 % of the total benthic  $\text{NO}_3^-$  consumption in the German Bight (Neumann et al., 2017).

64 Quantifying N dynamics based solely on changes in N concentrations provides limited insight into underlying  
65 reactions, as only net changes can be observed. Previous authors used different methods for determination of  
66 specific N rates. Lohse et al. (1993) used the acetylene block method, core flux incubations and isotope pairing in  
67 the early 1990s types to determine denitrification rates in a variety of sediment types (Tab. 1). Deek and co-authors  
68 (Deek et al., 2013; Deek et al., 2011) investigated N-turnover in the Wadden Sea and in the extended Elbe estuary  
69 using core flux incubations and isotope pairing. Marchant et al. (Marchant et al., 2016) measured denitrification  
70 rates in permeable sediments obtained from slurry incubations and percolated sediment cores. More recently,  
71 Neumann et al. (2017) used pore-water  $\text{NO}_3^-$  concentration gradient profiles to determine  $\text{NO}_3^-$  consumption rates  
72 in the German Bight.

73 Stable isotope techniques offer several approaches to quantify N turnover processes, and  $^{15}\text{N}$  tracer studies have  
74 been widely used to determine N transformation rates (e.g. nitrification and denitrification) (Brase et al., 2018;  
75 Sanders et al., 2018). The isotope dilution method can be used to distinguish between net and gross rates and so  
76 help to unravel several N-processes such as ammonification and assimilation or nitrification and denitrification.  
77  $^{15}\text{N}$  dilution (Koike and Hattori, 1978; Nishio et al., 2001) can be used to estimate gross N transformation rates  
78 by measuring the isotopic dilution of the substrate and product pools, respectively (e.g. Burger and Jackson, 2003).  
79 In this study, we used the isotope dilution method with labeled  $\text{NH}_4^+$  and  $\text{NO}_3^-$  in separate sediment cores to  
80 measure gross ammonification and gross nitrification. The net rates are determined by the sediment nutrient fluxes.  
81 To measure denitrification we determined the produced  $\text{N}_2$  independently of the labelling in the core. Sediment  
82 core incubation experiment setup can never reproduce the identical conditions related to the advective processes  
83 in permeable sediments. Nevertheless this method has advantages over just balancing sediment-water exchanges:  
84 (1) The appearance of  $^{15}\text{N}$  in the  $\text{NH}_4^+$  pool during the incubation allows an estimate of ammonification rates, (2)  
85 the isotopic dilution of  $\text{NO}_3^-$  tracks nitrification rates,

86 This study is conducted within the project “North Sea Observation and Assessment of Habitats” (NOAH). One  
87 important aspect of the project is to investigate the biogeochemical status and functions of the sea floor, especially  
88 nitrogen cycling, to gauge the eutrophication mitigation potential in light of continuing high human pressures  
89 (<https://www.noah-project.de>).

90 In this paper, we investigate internal N rates of ammonification, nitrification and denitrification at four stations  
91 across sediment types (clay/silt, fine sand, coarse sand) in the German Bight (North Sea) during late summer  
92 (August/September) 2016. To assess the internal sediment N processes and the rates of reactive N release to the  
93 water column, we incubated sediment cores amended with  $^{15}\text{NH}_4^+$  and  $^{15}\text{NO}_3^-$ . We quantify the benthic gross and  
94 net nitrification and ammonification rates and evaluate the environmental controls underlying spatial variabilities.  
95 We further discuss the role of ammonification as a source of reactive nitrogen for primary producers, of  
96 nitrification and of denitrification in the Southern North Sea.

## 97 **2 Material and Methods**

### 98 **2.1 Study site and sampling strategy**

99 The study site is in the German Bight (Southern North Sea), an area that is strongly influenced by nutrient inputs  
100 from large continental rivers. The salinity in the coastal zone of the North Sea ranges between ~30 and 35, and the  
101 average flushing time is 33 days (Lenhart and Pohlmann, 1997). The sampling was performed in August and  
102 September 2016 during R/V *Heincke* cruise HE-471 in the German Bight (Fig. 1).

103 The sampling sites are part of the NOAH (North Sea Assessment of Habitats) assessment scheme (Fig. 1). Samples  
104 were taken from 4 site (NOAH A, C, D and E) with different water depth and sediment characteristics (Table 2).  
105 The sites represent typical sediment types based on statistics of granulometric properties, organic matter content,  
106 permeability, and water depth assessed during former cruises (<https://doi.org/10.1594/PANGAEA.846041>).  
107 Organic matter and CN ratio data from cruises HE 383 (06/07.2012) and HE 447 (06.2015) were used.

### 108 **2.2 core sampling and incubation**

109 At each station (NOAH A, C,D and E) both water samples and sediment samples were taken. Water samples were  
110 taken with Niskin bottles attached to a CTD with additional chlorophyll and  $\text{O}_2$  sensors. Sediment multicores  
111 equipped with acrylic tubes (PMA) with an inner diameter of 10 cm and a length of 60 cm were used. Four intact  
112 sediment cores from each station (exception: Station NOAH-D, only 3 cores could successfully be retrieved) were  
113 incubated in a gas tight batch-incubation setup for 24 hours (Fig. 2) in the ship's laboratory at in-situ  
114 temperature (~19°C) directly after sampling. Cores were handled carefully to avoid disturbance that could alter  
115 benthic fluxes. Cores were incubated in the dark and the overlying site water was gently stirred with a magnetic  
116 stirrer, avoiding sediment resuspension. The overlying water column was adjusted to a height of 20 cm. Water  
117 temperature and oxygen concentration of the overlying water of sediment cores were measured continuously with  
118 optodes (PyroScience, Germany).

119 To measure gross ammonification, two sediment cores (Station NOAH-D 1 core only) were enriched with  $^{15}\text{NH}_4^+$   
120 (50 at-%), the other two cores were amended with  $^{15}\text{NO}_3^-$  (50 at-%) for an assessment of gross nitrification (Fig.

121 2).  $\text{NH}_4^+$  and  $\text{NO}_3^-$  concentrations of the added tracer solution were adjusted to bottom water concentrations based  
122 on nutrient data of previous cruises of the same location and time (later confirmed by nutrient analyses of site  
123 water). For label addition, site water was replaced with the respective label solution. Due to the careful adjustment  
124 of concentrations, incubations were done at a tracer level, and benthic fluxes should not be altered. The label  
125 addition was calculated aiming for a maximum enrichment of 5.000 ‰ in substrates and products.

126 Samples were taken every 6 hours. Upon sampling, incubation water was filtered with a syringe filter (cellulose  
127 acetate, Sartorius, 0.45  $\mu\text{m}$  pore size) and frozen in exetainers (11.8 ml, Labco, High Wycombe, UK) at  $-20^\circ\text{C}$  for  
128 later analyses of nutrients and stable isotope signatures ( $\delta^{15}\text{NH}_4^+$ ,  $\delta^{15}\text{NO}_3^-$ ). Additional samples for the analyses of  
129 dissolved nitrogen ( $\text{N}_2$ ) were taken without filtration, and were preserved in exetainers (5.9 ml, Labco, High  
130 Wycombe, UK) containing 2 % of a  $\text{ZnCl}_2$  solution (1 M). Samples were stored at  $4^\circ\text{C}$  under water until analysis.

### 131 **2.3 Analyses**

#### 132 **$\text{N}_2$ measurements by MIMS**

133  $\text{N}_2$  production was measured by a membrane inlet mass spectrometer (MIMS, inProcess Instruments), which  
134 quantifies changes in dissolved  $\text{N}_2:\text{Ar}$  ratios (Kana et al., 1994) from all four cores. During the measurements, the  
135 water samples were maintained in a temperature-controlled water bath ( $16^\circ\text{C}$ ). For calibration, we measured  
136 equilibrated water samples at four salinities, from 0 to 35 after each 10<sup>th</sup> water sample. We measured the production  
137 of  $^{28}\text{N}$ . The internal precision of the samples was  $<0.05\%$  for  $\text{N}_2/\text{Ar}$  analyses.

#### 138 **Oxygen penetration depth**

139 The oxygen penetration depth in the sediment of each station was measured using microoptodes (50  $\mu\text{m}$  tip size;  
140 Presens, Germany). The optodes were moved vertically into the sediment with a micromanipulator (PyroScience,  
141 Germany), in steps of 100-200  $\mu\text{m}$ , depending on the oxygen concentration. Three  $\text{O}_2$  profiles were measured in  
142 one sediment core of each station. The  $\text{O}_2$  profiles were measured directly after core retrieval, i.e. within 10 – 15  
143 minutes.

#### 144 **Sediment samples**

145 The surface sediment samples (first 1 cm) of the cruises HE 383 (06/07-2012) and HE 447 (06-2015) were  
146 analyzed for total carbon and total nitrogen contents with an elemental analyzer (Carlo Erba NA 1500) The total  
147 organic carbon content was analyzed after removal of inorganic carbon using 1 mol  $\text{L}^{-1}$  hydrochloric acid. The  
148 standard deviation of sediment samples was better than 0.6 % for  $\text{C}_{\text{org}}$  and 0.08 % for N determination.

149 Permeability and porosity of the sediments were conducted with sediments from the cruise He-471, the methods  
150 were described in detail elsewhere (Neumann, 2016).

#### 151 **Dissolved inorganic nitrogen concentrations**

152 NO<sub>x</sub>, NO<sub>2</sub><sup>-</sup> and NH<sub>4</sub><sup>+</sup> concentrations of the water column samples were determined in replicate with a continuous  
153 flow analyzer (AA3, Seal Analytics, Germany) according to standard colorimetric techniques (NO<sub>x</sub>, NO<sub>2</sub>:  
154 (Grasshoff et al., 1999), NH<sub>4</sub><sup>+</sup>: (K erouel and Aminot, 1997)). NO<sub>3</sub><sup>-</sup> concentration was calculated by difference  
155 between NO<sub>x</sub> and NO<sub>2</sub><sup>-</sup>. Based on replicate analyses, measurement precision for NO<sub>x</sub> and NO<sub>2</sub><sup>-</sup> was better than 0.1  
156  mol L<sup>-1</sup> and better than 0.2  mol L<sup>-1</sup> for NH<sub>4</sub><sup>+</sup>.

157 Water samples from core incubations were analyzed in duplicate for concentration of NH<sub>4</sub><sup>+</sup>, NO<sub>2</sub><sup>-</sup> and NO<sub>3</sub><sup>-</sup> using  
158 a multimode microplate reader Infinite F200 Pro and standard colorimetric techniques (Grasshoff et al., 1999) at  
159 the ZMT, Bremen. The standard deviations were <1  mol L<sup>-1</sup> for NO<sub>3</sub><sup>-</sup>, <0.2  mol L<sup>-1</sup> for NO<sub>2</sub><sup>-</sup> and <0.5  mol L<sup>-1</sup>  
160 for NH<sub>4</sub><sup>+</sup>.

#### 161 **Nitrogen isotope analyses**

162 The nitrogen isotope ratios of NO<sub>3</sub><sup>-</sup> were determined via the denitrifier method (Casciotti et al., 2002; Sigman et  
163 al., 2001). This method is based on the mass spectrometric measurement of isotopic ratios of N<sub>2</sub>O produced by the  
164 bacterium *Pseudomonas aureofaciens*. Briefly, 20 nmoles of sample NO<sub>3</sub><sup>-</sup> were injected in a 20 ml vial containing  
165 MilliQ. Two international standards were used (IAEA-NO<sub>3</sub><sup>-</sup>  <sup>15</sup>N = +4.7 ‰, USGS-34  <sup>15</sup>N = -1.8 ‰) for a  
166 regression-based correction of isotope values. For further quality assurance, an internal standard was measured  
167 with each batch of samples. The standard deviation for  <sup>15</sup>N was better than <0.2 ‰

168 For ammonium isotope measurements, nitrite was removed by reduction with sulfamic acid (Granger and Sigman,  
169 2009) before NH<sub>4</sub><sup>+</sup> was chemically oxidized to NO<sub>2</sub><sup>-</sup> by hypobromite at pH ~12 and then reduced to N<sub>2</sub>O using  
170 sodium azide (Zhang et al., 2007). 10 nmol of NH<sub>4</sub><sup>+</sup> were injected, and all samples with [NH<sub>4</sub><sup>+</sup>] >1  mol L<sup>-1</sup> were  
171 analyzed. For the calibration of the ammonium isotopes, we used three international standards (IAEA-N1  <sup>15</sup>N =  
172 +0.4 ‰, USGS 25  <sup>15</sup>N = -30.4 ‰, USGS 26  <sup>15</sup>N = +53.7 ‰). The standard deviations were better than 1 ‰.

173 N<sub>2</sub>O produced either by the denitrifier method or the chemical conversion of ammonium was analysed with a  
174 GasBench II, coupled to an isotope ratio mass spectrometer (Delta Plus XP, Thermo Fisher Scientific).

#### 175 **2.4. Rates and fluxes calculation for respiration, ammonification, nitrification and denitrification rates in** 176 **core incubations**

##### 177 Benthic fluxes

178 Oxygen consumption, net ammonification, net nitrification and denitrification were calculated based on  
179 concentration changes in the sediment incubations. The respective benthic fluxes were calculated as follows:

$$180 r_{\text{net}} = d(C) \cdot V / d(t) \cdot A \text{ [mmol N m}^{-2} \text{ d}^{-1}] \quad (1)$$

181 where  $d(C)$  is the oxygen, nutrient or the nitrogen ( $N_2$ ) concentration at the start and at the end of the experiment,  
182  $V$  is the volume of the overlying water,  $d(t)$  is the incubation time and  $A$  is the surface area of the sediment..  
183 Positive fluxes (outflow concentrations above inflow concentrations) imply net production in the sediment.

#### 184 Gross rates of ammonification and nitrification

185 Gross rates of ammonification and nitrification ( $r_{\text{gross}}$ ) were calculated based on  $^{15}\text{N}$  isotope dilution (Koike and  
186 Hattori, 1978; Nishio et al., 2001). For example, ammonification rates are calculated based on  $^{15}\text{NH}_4^+$  additions,  
187 nitrification rates are based on  $^{15}\text{NO}_3^-$  additions (Fig. 2) :

$$188 \quad r_{\text{gross}} = [\ln(f^{15}\text{N}_{\text{end}}/f^{15}\text{N}_{\text{start}})]/[\ln(C_{\text{end}}/C_{\text{start}})]*(C_{\text{start}}-C_{\text{end}}/t)*(V/A*\Delta t) \quad (2)$$

189 where  $C_{\text{start}}$  is the initial  $\text{NH}_4^+$  or  $\text{NO}_3^-$  concentration,  $C_{\text{end}}$  is the concentration at time  $t$ , and  $f^{15}\text{N}_{\text{start}}$  and  $f^{15}\text{N}_{\text{end}}$   
190 represent  $^{15}\text{N}$  atom% excess (Brase et al., 2018),  $V$  is the volume of the overlying water and  $A$  is the surface area  
191 of the sediment. All rates are given in  $\text{mmol N m}^{-2} \text{d}^{-1}$

### 192 **3 Results**

#### 193 *Ammonification*

194 We measured gross ammonification rates with the isotope dilution method using  $^{15}\text{NH}_4^+$  as tracer, and measured  
195 net ammonium fluxes with the flux method. The highest net ammonium flux and gross ammonification rates were  
196 measured in the impermeable, organic-rich sediment at station NOAH-C ( $6.6 \pm 1.4 \text{ mmol N m}^{-2} \text{d}^{-1}$  and  $9.5 \text{ mmol}$   
197  $\text{N m}^{-2} \text{d}^{-1}$  for net flux and gross ammonification, respectively).

198 The lowest net ammonium fluxes were measured in the semi-impermeable sediment at station NOAH-D ( $0.5 \pm$   
199  $0.1 \text{ mmol N m}^{-2} \text{d}^{-1}$ ). The lowest gross ammonification rate was measured at the permeable sediment station  
200 NOAH-A ( $2.1 \pm 0.3 \text{ mmol N m}^{-2} \text{d}^{-1}$ ). The impermeable sediment station NOAH-C had the highest net ammonium  
201 fluxes ( $6.6 \pm 1.4 \text{ mmol N m}^{-2} \text{d}^{-1}$ ) and gross ammonification rates ( $9.5 \text{ mmol m}^{-2} \text{d}^{-1}$ ). Net and gross ammonification  
202 rates are significantly correlated ( $r^2=0.55$ ; see electronic supplemental).

#### 203 *Nitrification*

204 Likewise to ammonification, we measured gross nitrification rates by means of the stable isotope dilution method  
205 with  $^{15}\text{NO}_3^-$  as tracer, and net nitrate fluxes employing the flux method. Net fluxes and gross nitrification rates  
206 varied significantly between stations. Net nitrate fluxes were highest at station NOAH-C and at station NOAH-E  
207 with  $1.1 \pm 0.5 \text{ mmol N m}^{-2} \text{d}^{-1}$  and  $1.2 \pm 0.5 \text{ mmol N m}^{-2} \text{d}^{-1}$ , respectively (Fig. 3, Fig. 5). Gross nitrification rates  
208 were highest at NOAH-C ( $2.1 \pm 0.1 \text{ mmol N m}^{-2} \text{d}^{-1}$ ). The lowest rates of net nitrate flux ( $0.3 \pm 0.3 \text{ mmol N m}^{-2} \text{d}^{-1}$ )  
209 and gross nitrification ( $1.2 \pm 0.0 \text{ mmol m}^{-2} \text{d}^{-1}$ ) were observed in the permeable sediment at station NOAH-A.  
210 Net and gross nitrification rates are closely correlated ( $r^2=0.87$ ; Fig. 3) with net nitrate fluxes being systematically  
211 lower than gross nitrification rates.

## 212 *Denitrification*

213 Unlike to ammonification and nitrification, we were not able to make use of the stable isotope tracers to evaluate  
214  $N_2$  production rates with an stable isotope technique because the requirements for the Isotope Pairing method  
215 (Rysgaard-Petersen et al., 1996) were not met. Our  $N_2$  production estimates are thus limited to the flux method.  
216 The observed average denitrification rates ranged from  $1.3 \pm 1.1 \text{ mmol N m}^{-2} \text{ d}^{-1}$  to  $1.9 \pm 0.8 \text{ mmol N m}^{-2} \text{ d}^{-1}$   
217  $\text{N m}^{-2} \text{ d}^{-1}$  (Fig. 5) and did not vary significantly between stations.

## 218 **Sedimentary organic matter descriptions**

219 The data show a clear correlation between sediment type and organic carbon and nitrogen content. Clay and silty  
220 sediment (NOAH-C) had the highest organic carbon (0.73 %) and nitrogen (0.10 %) concentrations (Tab. 2).  
221 Medium sand station (NOAH-A) had the lowest  $C_{\text{org}}$  (0.03 to 0.04 %) and total nitrogen (<0.01 to 0.01 %)  
222 concentrations. This trend does probably not apply to NOAH-E since the samples for C / N analyses were retrieved  
223 prior to the abrupt emergence of a large pockmark field at this station (Krämer et al. 2017) while the sediment  
224 cores for the incubations were retrieved after the emergence of the pockmarks. The large scale sediment  
225 resuspension event resulted in numerous newly formed depressions with increased sedimentation of organic  
226 material.

227

## 228 **4 Discussion**

### 229 **4.1 Magnitude and relevance of ammonification**

230 A principal goal of this study was to assess the role of ammonification in the nitrogen cycle of the German Bight.  
231 Ammonification releases  $NH_4^+$  during the decomposition of organic matter and resupplies the water-column  
232 inventory of reactive nitrogen. The quantification of ammonification rates is challenging, because ammonium is  
233 readily assimilated by primary producers or is rapidly nitrified, causing low ammonium concentrations and  
234 necessitating to use the isotope dilution method.

235 This study represents direct measured gross ammonification rates across typical sediment types of the North Sea,  
236 covering a large range from 1.9 to 9.5  $\text{mmol N m}^{-2} \text{ d}^{-1}$ : Ammonification rates were mainly governed by sediment  
237 texture and organic matter content. The impermeable muddy sediment at station NOAH-C with high  $C_{\text{org}}$  and TN  
238 content (0.73 % and 0.10 %, respectively, Tab. 2) had highest gross and net ammonification rates. This is line with  
239 other studies showing enhanced ammonium release in muddy coastal sediments (e.g. Caffrey, 1995).

240 The sandy sediments at sites NOAH-A, NOAH-D and NOAH-E exhibited significantly lower gross  
241 ammonification rates. This reflects the lower sediment organic matter content in these sandy sediments expressed  
242 in  $C_{\text{org}}$  (0.03 – 0.04 %) and N (0.01 – <0.01 %) concentrations (Caffrey, 1995), Tab. 2).



243 It is striking, though, that net and gross ammonification in the sandy sediment at station NOAH-E was clearly  
244 elevated compared to the other sandy stations NOAH-A and NOAH-D. There are two possible explanations for  
245 this enhanced ammonium production: (1) enhanced supply of organic matter to the sediment surface or (2) effects  
246 bioirrigation and bioturbation.

247 Station NOAH-E is located inside a pockmark field that had developed relatively recently, between July and  
248 November 2015 (Krämer et al., 2017). Our assessment of C and N content is based on samples that were taken  
249 prior to the pockmark formation in 2012 and 2015 (<https://doi.org/10.1594/PANGAEA.883199>). The sediment  
250 samples during the cruise (He-471) in 2016 were taken from the depression inside an individual pockmark, which  
251 was about ~0.2 deeper than the surrounding sediment (Krämer et al., 2017). We assume that organic matter from  
252 the water column accumulated in these transient structures, and that the organic carbon and nitrogen content thus  
253 was elevated. A transient change in surface sediment composition, which is not captured by our compositional  
254 data, may thus have caused the enhanced ammonification rate.

255 An alternative explanation is an elevation of ammonium fluxes from the sediment due to sediment reworking. In  
256 the sediment incubations, we found a high benthic activity of *Spiophanes bombyx* and *Phoronis sp.*. Both benthic  
257 organisms can increase the nutrient fluxes from the sediment to the bottom water, the oxygen penetration depth,  
258 and, in turn, organic matter degradation in the oxic zone (Aller, 1988).

259 Under completely oxic conditions, the ratio of  $\text{NH}_4^+$  release and  $\text{O}_2$  consumption in the entire study area should  
260 approximate Redfield ratios of about 1:8.6 (Thibodeau et al., 2010). Such ratios were observed at the semi-  
261 permeable station NOAH-D, the permeable station NOAH-A (Fig. 2), and at station NOAH-E, suggesting that in  
262 these cores most of the organic matter was degraded under oxic conditions. At station NOAH-C, however, the  
263 N: $\text{O}_2$  ratio was clearly elevated above the Redfield ratio. While this finding is based on an individual assessment,  
264 it appears plausible: We presume that the enhanced production of ammonium relative to  $\text{O}_2$  consumption reflects  
265 the importance of anoxic ammonium generation, i.e., during methanogenesis or sulfate reduction (e.g. Jorgensen,  
266 1982). This is quite likely at station NOAH-C, where oxygen penetration depth in the impermeable, organic-rich  
267 sediment is lowest, and where increasing  $\text{NH}_4^+$  concentrations with depth indicate decomposition or organic matter  
268 in the absence of free oxygen (Hartmann et al., 1973).

#### 269 **4.2 Ammonification coupled to denitrification by nitrification**

270 Based on the interpolation of gross rates of ammonification, it is evident that ammonification contributes  
271 significantly to nutrient regeneration in the German Bight. However, there is a clear difference between gross and  
272 net ammonification rates, suggesting that ammonium is taken up, either by assimilation or nitrification. In dark

273 sediments, where phototrophic organisms are light limited, we presume that nitrification is likely the more  
274 important process (Dähnke et al., 2012).

275 Nitrification produces  $\text{NO}_3^-$ , which represents the largest DIN pool in the water column of the North Sea and is the  
276 substrate for denitrification, and thus the link to an ultimate removal of fixed nitrogen from the water column.

277 We observed gross nitrification rates at all four stations ranging from  $1.2 \pm 0.0 \text{ mmol N m}^{-2} \text{ d}^{-1}$  at the sandy station  
278 NOAH-A, to  $1.3 \text{ mmol N m}^{-2} \text{ d}^{-1}$  in the moderately permeable sediment at NOAH-D and to  $2.1 \pm 0.1 \text{ mmol N m}^{-2}$   
279  $\text{d}^{-1}$  in the impermeable sediment at station NOAH-C (Fig. 3, Fig. 5). Gross nitrification at the impermeable  
280 sediment station NOAH-C accounted for around 22.2 % ( $\pm 0.7$  %), around 38.5 % at the semi-permeable station  
281 (NOAH-D) and around 50.6 % ( $\pm 15.8$  %) at the permeable sediment stations of total DIN flux to the bottom water.  
282 Overall, nitrification is in the same range as reported by Marchant et al. (2016) in sandy sediment near Helgoland  
283 ( $0.2$  to  $3.0 \text{ mmol m}^{-2} \text{ d}^{-1}$ ; Tab. 1). Highest nitrate fluxes from the sediment and gross nitrification rates were  
284 observed at the impermeable station NOAH-C and at station NOAH-E, where pockmark structure and organic  
285 matter accumulation might have affected benthic nutrient fluxes (see section 4.1).

286 Lowest gross nitrification rates and nitrate fluxes are found at the permeable station NOAH-A, but apart from this,  
287 we do not see a clear correlation of nitrification and permeability in our study. Nonetheless, nitrification rates are  
288 lowest at Station NOAH-A, where oxygen penetration depth is highest, and the sediment has low organic matter  
289 content (Tab. 2). A high oxygen penetration depth can support nitrification, but it is in this case obviously substrate  
290 limited due to low organic matter content, which limits ammonification. Oxygen penetration can enhance  
291 nitrification at greater depth, but can, on the other hand, also increase diffusion limitation (Alkhatib et al., 2012).  
292 Due to this dual control of nitrification by OPD on the one hand and substrate availability on the other, the  
293 individual correlations between  $C_{\text{org}}$  or TN and nitrification are relatively weak. Generally, organic matter  
294 deposition in the sediment supports higher ammonification rates, which in turn enhance nitrification under oxic  
295 conditions (Henriksen and Kemp, 1988; Rysgaard et al., 1996). Consequently, nitrification is affected by the  $\text{NH}_4^+$   
296 pool in the sediment, temperature, salinity and  $\text{O}_2$  (e.g. Sanders, 2018).

297 This interplay of factors is mirrored in a clear and statistically significant ( $\alpha=0.05$ ) correlation of gross nitrification  
298 and gross ammonification rates ( $r^2 = 0.92$ ). Overall, the gross  $\text{NO}_3^-$  production ( $1.2$  to  $2.1 \text{ mmol m}^{-2} \text{ d}^{-1}$ ) was small  
299 relative to ammonification rates ( $1.9$  to  $9.5 \text{ mmol N m}^{-2} \text{ d}^{-1}$ ). We find that nitrification is governed by a complex  
300 interplay of variables such as ammonification rate, permeability, organic matter availability and oxygen  
301 penetration depth, and is likely difficult to predict based on one of these factors alone. Generally, organic matter  
302 deposition in the sediment supports higher ammonification rates, which in turn enhance nitrification under oxic

303 conditions (Henriksen and Kemp, 1988; Rysgaard et al., 1996). In our setting, this is reflected in a clear correlation  
304 of gross rates of ammonification and nitrification.

### 305 **4.3 Denitrification**

306 Denitrification, the reduction of  $\text{NO}_3^-$  to gaseous  $\text{N}_2$ , reduces the pool of bioavailable N, and is therefore very  
307 relevant in eutrophic coastal areas such as the southern North Sea. In our study, the measured denitrification rates  
308 ranged from 1.3 to 1.9  $\text{mmol N m}^{-2} \text{d}^{-1}$  (Fig. 5). This estimate is on the higher end of previous measurements from  
309 sites in the German Bight (Deek et al., 2013; Marchant et al., 2016) (Tab. 1), but generally fits with previous  
310 observations. We assume that the rates in our study are elevated because sampling took place after the spring  
311 phytoplankton bloom, and not all organic matter that had been deposited at the sediment surface had been  
312 remineralized. Such a decoupling of water column production and sedimentary denitrification has been observed  
313 before in stratified water masses of the Baltic Sea (Hellemann et al., 2017). Even though our study was designed  
314 to cover diverse sediment types, and thus allow for an improved extrapolation of rates to the total German Bight  
315 area, this highlights the heterogeneity of sediments, and points out that the sampling season can have a marked  
316 effect on measured rates. Therefore, follow-up experiments should try to cover the seasonality as much as possible  
317 to improve estimates of denitrification in the German Bight area.

318 Important seasonal effects on denitrification can be attributed to variations in oxygen supply, changing bottom  
319 water  $\text{NO}_3^-$  concentration and organic carbon content in the sediment (Deek et al., 2013). In our study, the bottom  
320 water nitrate concentration is too low ( $<0.5$  to  $4.5 \mu\text{mol L}^{-1}$ ) to sustain the observed denitrification rates, and thus  
321 the major nitrate source fueling the observed denitrification must be coupled nitrification-denitrification fueled by  
322 mineralization of sedimentary organic material. This is reflected in a strong correlation between gross nitrification  
323 and denitrification rates ( $r^2 = 0.85$ ).

324 In our study, we find that this coupled nitrification-denitrification determines the total N flux. Denitrification  
325 essentially removes, within the given uncertainties (Fig. 5) all nitrate produced by nitrification at study sites  
326 NOAH-A and NOAH-D. At stations NOAH-C and NOAH-E, where we assume a (possibly transient in case of  
327 NOAH-E) accumulation of organic matter, nitrification rates are enhanced, and a substantial amount of freshly  
328 produced nitrate is released to the water column.

329 In comparison to the supply of mineralized N (i.e., gross ammonification) denitrification accounts for ~20 % (1.9  
330  $\text{mmol N m}^{-2} \text{d}^{-1} / 9.5 \text{mmol N m}^{-2} \text{d}^{-1}$ ) at the impermeable sediment station NOAH-C, ~39 % (1.3  $\text{mmol N m}^{-2} \text{d}^{-1}$   
331 / 3.3  $\text{mmol N m}^{-2} \text{d}^{-1}$ ) at the semi-permeable sediment station NOAH-D and ~ 62 % (1.3  $\text{mmol N m}^{-2} \text{d}^{-1} / 2.1$   
332  $\text{mmol N m}^{-2} \text{d}^{-1}$ ) at permeable sediment stations (NOAH-A). As discussed above, this trend does not hold for the  
333 less representative station NOAH-E due to the transient formation of numerous pockmarks.

#### 334 4.4 Significance of benthic N-recycling

335 Our study covers the most sediment types across the German Bight, but is based on core incubations and therefore  
336 potentially underestimates advective processes. In a recent study by Neumann et al. (2017), the authors used  $\text{NO}_3^-$   
337 pore water profiles to calculate the  $\text{NO}_3^-$  consumption rates across a similar range of North Sea sediments. They  
338 extrapolated their nitrate consumption rates to the entire area of the German Bight based on a permeability  
339 classification of sediments. They propose that ~24 % of sediments in the southern North Sea (German Bight) are  
340 impermeable sediments (12,200  $\text{km}^2$ ), ~39 % are moderately permeable sediments (19,600  $\text{km}^2$ ) and ~37 %  
341 (18,800  $\text{km}^2$ ) are permeable sediments. They estimated that permeable sediment were the most efficient  $\text{NO}_3^-$  sink  
342 accounting for up to 90 % of the total benthic  $\text{NO}_3^-$  consumption. In our assessment, which better represents the  
343 role of nitrification, we arrive at a somewhat lower contribution of ~68 % of total denitrification occurring in  
344 moderately permeable and permeable sediments. Based solely on our data, we estimate a total nitrogen removal  
345 of ~1030  $\text{t N d}^{-1}$  in our study area, which corresponds to an average  $\text{N}_2$  flux of approximately  $1.5 \text{ mmol N m}^{-2} \text{ d}^{-1}$ .  
346 This daily  $\text{N}_2$  production during late summer equals the total N discharge (~1.000  $\text{t N d}^{-1}$ ) by the main rivers Maas,  
347 Rhine, North-Sea Canal, Ems, Weser and Elbe (Pätsch and Lenhart, 2004), and, as such, underscores the role of  
348 coastal sediments to counteract the eutrophication in the North Sea.

349 Our assessment, however, does reflect the impact of only diffusive transport and faunal activity while not  
350 accounting for advective fluxes. Based on the same data set of permeability for classification of different sediment  
351 types that Neumann et al. (2017) used, we will merge our dataset with the results of Neumann et al. (in preparation)  
352 to arrive at an improved estimate of sediment denitrification that includes benthic nitrification as a nitrate source.  
353 In the following, we aim to put our estimates of N-transition rates into perspective by setting an upper limit of N  
354 turnover based on primary production since N cycling is linked to organic carbon availability, which is ultimately  
355 provided by pelagic primary production. For the freshwater influenced regions of the German Bight, Capuzzo et  
356 al. (2018) assume a C fixation of  $1.05 \text{ g C m}^{-2} \text{ d}^{-1}$ . For an estimate of the maximum N transition rate we assume  
357 that 10 % of the fixed C is processed in the sediment (Heip et al., 1995) and that all carbon is remineralized in the  
358 sediment in pace with N turnover. Based on Redfield stoichiometry (~12 g / mol C, ~14 g / mol N), average C  
359 fixation translates to  $[1.05 \text{ g} * 10 \% / 12 \text{ C} * 14\text{N} =] 0.123 \text{ mg N}$  that is removed per  $\text{m}^{-2}$  and day, or  $9 \text{ mmol N m}^{-2}$   
360  $\text{d}^{-1}$ , respectively. This sets an upper limit to the N turnover rate and compares well with the observed  
361 ammonification rate in impermeable sediment at NOAH-C ( $9.5 \text{ mmol NH}_4^+ \text{ m}^{-2} \text{ d}^{-1}$ , Figure 5). The ammonification  
362 rates at the sandy stations are substantially lower, which certainly reflects that sandy sediments are frequently  
363 resuspended and organic particles are resuspended and degraded in the water column. For a second line of  
364 argument, we consider the annual nitrate budget of the southern North Sea (Hydes et al. 1999, van Beusekom et

365 al. 1999) with an annual average denitrification rate of  $0.7 \text{ mmol N m}^{-2} \text{ d}^{-1}$ . This value agrees well with the average  
366 gap of  $0.5 \text{ mmol N m}^{-2} \text{ d}^{-1}$  between gross nitrification and actual nitrate flux (Figure 4), which we attribute to  
367 denitrification. Both rates, the budget-based estimate and the nitrification gap are in the lower range of our  
368 measured  $\text{N}_2$  fluxes of  $0.3$  to  $2.9 \text{ mmol N m}^{-1} \text{ d}^{-1}$  (Tab. 1, Fig. 5). For a third line of argument, we employ the  
369 approach of Seitzinger and Giblin (1996) to link benthic respiration and denitrification directly to the pelagic  
370 primary production. By employing their formulas and using the primary production rates by Capuzzo et al. (2018),  
371 the annual average of the sediment oxygen demand would be  $14.3 \text{ mmol O}_2 \text{ m}^{-2} \text{ d}^{-1}$  ( $1.05 \text{ g C d}^{-1} \text{ m}^{-2} = 87.5 \text{ mmol}$   
372  $\text{C d}^{-1} \text{ m}^{-2}$ ), which corresponds to a benthic denitrification rate of  $3.3 \text{ mmol N m}^{-2} \text{ d}^{-1}$ . Since the annual average of  
373 actually measured oxygen fluxes are close to this estimate ( $15.4 \pm 12.9 \text{ mmol O}_2 \text{ m}^{-2} \text{ d}^{-1}$ ,  $N=175$ ) (Neumann et al.,  
374 in preparation), we are confident that our denitrification estimates of up to  $2.9 \text{ mmol N m}^{-2} \text{ d}^{-1}$  are reasonable.  
375 However, with the multitude of our approaches yielding quite a span of plausible denitrification estimates the  
376 question emerges which of the figures in the range of  $0.5$  to  $3.3 \text{ mmol N m}^{-1} \text{ d}^{-1}$  is actually the true value for the  
377 average denitrification rate. One major reason for this level of uncertainty is the fact that the local sediment  
378 properties with regard to macrofauna composition and organic matter content varied considerably within each  
379 station, which is reflected e.g. in the variability of oxygen consumption rates (see electronic supplemental). Since  
380 we were restricted to 4 cores per station in total, and just 2 cores for labelling with  $^{15}\text{NH}_4^+$  and  $^{15}\text{NO}_3^-$ , respectively,  
381 the inevitable spatial heterogeneity introduced a substantial degree of random error. Additionally, the preceding  
382 results we used above to evaluate our observations are certainly likewise based on imperfect data, which results in  
383 uncertainty on that side. In summary, our limited set of new observations is not sufficiently large to favor one of  
384 the preceding denitrification estimates. At least, the average of all our  $\text{N}_2$  measurements of  $1.5 \pm 0.9 \text{ mmol N m}^{-2}$   
385  $\text{d}^{-1}$  ( $N=13$ ) falls right in the center of the interval of  $0.5$  to  $3.3 \text{ mm}$  and might represent our best estimate for an  
386 average denitrification rate in late summer. The remaining fraction of the initial ammonification is recycled back  
387 into the water column as DIN, which accounts for  $69 \pm 18 \%$  ( $N=12$ ) of the total benthic N flux ( $\text{N}_2 + \text{DIN}$ ).  
388 Since benthic N recycling substantially restocks the pelagic N inventory, we further assessed the contribution of  
389 benthic N recycling by comparing the benthic DIN (ammonium + nitrite + nitrate) fluxes with the inventory of  
390 DIN below the thermocline. Assuming steady state, we find a rapid turnover of sediment-derived DIN at NOAH-  
391 C and NOAH-E, in the range of 1-3 days (Tab. 3). This implies that even below the thermocline, DIN derived by  
392 the sediment is rapidly assimilated by phytoplankton. Previous publications showed that primary production below  
393 the thermocline contributes  $\sim 37 \%$  to total primary production in the North Sea (van Leeuwen et al., 2013).  
394 Assuming Redfield stoichiometry and an average primary production of  $1.05 \text{ g C m}^{-2} \text{ d}^{-1}$ , benthic DIN fluxes in  
395 our measurements can support a primary production of about  $6.2$  to  $51.4 \text{ mmol C m}^{-2} \text{ d}^{-1}$  or  $74 - 617 \text{ mg C m}^{-2}$

396 day<sup>-1</sup>. This is within the range of previously observed and modeled primary production rates in the North Sea  
397 during summer (e.g. van Leeuwen et al., 2013). We further estimate that depending on the thickness of the bottom  
398 water layer below the thermocline, benthic N fluxes during the sampling time supported between  $7.1 \pm 2.6$  % (38  
399 m bottom water layer) and  $58.7 \pm 10.6$  % (10 m bottom water layer) of the annual average of primary production  
400 (Tab. 3). This dependence of relative sediment contribution on water depth has been observed previously for  
401 respiration processes (Heip et al., 1995). Our data also match the calculation of Blackburn and Henriksen (1983)  
402 for Danish sediments, where N fluxes could support 30 to 83 % of the nitrogen requirement of the planktonic  
403 primary producers (Blackburn and Henriksen, 1983).

404

## 405 **5 Summary and concluding remarks**

406 We evaluated a range of sedimentary nitrogen turnover pathways and found that ammonification in sediments is  
407 an important N-source for primary production in the water column of the southeastern North Sea during summer.  
408 Depending on water depth, 7.1 to 58.7 % of the estimated water column primary production is fueled by  
409 sedimentary N release. Nitrification act as the main sinks of  $\text{NH}_4^+$  mineralized from sedimentary organic matter.  
410 Ultimately, the main factors governing nitrification are organic matter content / ammonification and oxygen  
411 penetration depth in the sediment. The share of newly produced  $\text{NO}_3^-$  reduced to  $\text{N}_2$  amounts to two thirds of  $\text{NO}_3^-$   
412 in permeable sediments, to nearly one half in moderately permeable sediment, and to one third in impermeable  
413 sediments. We further showed that moderately permeable and permeable sediments account for up to ~80 % of  
414 the total benthic  $\text{N}_2$  production ( $\sim 1030 \text{ t N d}^{-1}$ ) in the southern North Sea (German Bight) during the peak of benthic  
415 activity in late summer. Only then, benthic  $\text{N}_2$  production can compensate the annually averaged daily N input by  
416 the main rivers (e.g. Elbe, Ems, Rhine, Weser) discharging into the southern North Sea ( $\sim 1.000 \text{ t N d}^{-1}$ ). Thus  
417 impermeable sediments act as an important N source for primary producers, whereas moderately permeable and  
418 permeable sediments comprise a main reactive N sink counteracting eutrophication in the North Sea. Seasonal and  
419 spatial variabilities, especially from nearshore to offshore, should be evaluated in future studies.

420

## 421 **Acknowledgements**

422 We thank the captain and the crew of *R/V Heincke* for their support during the sampling campaigns. M. Birkicht  
423 from the Leibniz Centre for Tropical Marine Research (ZMT) in Bremen is gratefully acknowledged for his  
424 assistance with nutrient measurements. We further thank E. Logemann for the analysis of macrobenthos.

425 **References**

- 426 Alkhatib, M., Lehmann, M. F., and del Giorgio, P. A.: The nitrogen isotope effect of benthic  
427 remineralization-nitrification-denitrification coupling in an estuarine environment, *Biogeosciences*, 9,  
428 1633-1646, 2012.
- 429 Aller, R. C.: Benthic Fauna and Biogeochemical Processes in Marine Sediments: The Role of Burrows  
430 Structures. In: *Nitrogen cycling in Coastal Marine Environments*, Blackburn, T. H. and Sørensen, J.  
431 (Eds.), Scope, Chichester, 1988.
- 432 Bale, N. J., Villanueva, L., Fan, H., Stal, L. J., Hopmans, E. C., Schouten, S., and Sinninghe Damste, J. S.:  
433 Occurrence and activity of anammox bacteria in surface sediments of the southern North Sea, *FEMS*  
434 *Microbiol Ecol*, 89, 99-110, 2014.
- 435 Blackburn, T. H. and Henriksen, K.: Nitrogen cycling in different types of sediments from Danish  
436 waters, *Limnology and Oceanography*, 28, 477-493, 1983.
- 437 Brase, L., Sanders, T., and Daehnke, K.: Anthropogenic changes of nitrogen loads in a small river:  
438 external nutrient sources vs. internal turnover processes, *Isotopes in Environmental and Health*  
439 *Studies*, 54, 168-184, 2018.
- 440 Burger, M. and Jackson, L. E.: Microbial immobilization of ammonium and nitrate in relation to  
441 ammonification and nitrification rates in organic and conventional cropping systems, *Soil Biology and*  
442 *Biochemistry*, 35, 29-36, 2003.
- 443 Cadée, G. C. and Hegemann, J.: Phytoplankton in the Marsdiep at the end of the 20th century; 30  
444 years monitoring biomass, primary production, and Phaeocystis blooms, *Journal of Sea Research*, 48,  
445 97-110, 2002.
- 446 Caffrey, J. M.: Spatial and Seasonal Patterns in Sediment Nitrogen Remineralization and Ammonium  
447 Concentrations in San Francisco Bay California, *Estuarine, Coastal and Shelf Science*, 18, 219-233,  
448 1995.
- 449 Capuzzo, E., Lynam, C. P., Barry, J., Stephens, D., Forster, R. M., Greenwood, N., McQuatters-Gollop,  
450 A., Silva, T., van Leeuwen, S. M., and Engelhard, G. H.: A decline in primary production in the North  
451 Sea over 25 years, associated with reductions in zooplankton abundance and fish stock recruitment,  
452 *Glob Chang Biol*, 24, e352-e364, 2018.
- 453 Casciotti, K. L.: Nitrogen and Oxygen Isotopic Studies of the Marine Nitrogen Cycle, *Ann Rev Mar Sci*,  
454 8, 379-407, 2016.
- 455 Casciotti, K. L., Sigman, D. M., Hastings, M. G., Böhlke, J. K., and Hilkert, A.: Measurement of the  
456 oxygen isotopic composition of nitrate in seawater and freshwater using the denitrifier method, *Anal.*  
457 *Chem.*, 74, 4905-4912, 2002.
- 458 Dähnke K., Moneta A., Veuger B., Soetaert K., Middelburg J.J.: Balance of assimilative and  
459 dissimilative nitrogen processes in a diatom-rich tidal flat sediment. *Biogeosciences*. 2012;9:4059-70,  
460 2012.
- 461 Deek, A., Dähnke, K., van Beusekom, J., Meyer, S., Voss, M., and Emeis, K.: N<sub>2</sub> fluxes in sediments of  
462 the Elbe Estuary and adjacent coastal zones, *Marine Ecology Progress Series*, 493, 9-21, 2013.
- 463 Deek, A., Emeis, K., and van Beusekom, J.: Nitrogen removal in coastal sediments of the German  
464 Wadden Sea, *Biogeochemistry*, 108, 467-483, 2011.
- 465 Emeis, K.-C., van Beusekom, J., Callies, U., Ebinghaus, R., Kannen, A., Kraus, G., Kröncke, I., Lenhart,  
466 H., Lorkowski, I., Matthias, V., Möllmann, C., Pätsch, J., Scharfe, M., Thomas, H., Weisse, R., and  
467 Zorita, E.: The North Sea — A shelf sea in the Anthropocene, *Journal of Marine Systems*, 141, 18-33,  
468 2015.
- 469 Granger, J. and Sigman, D. M.: Removal of nitrite with sulfamic acid for nitrate N and O isotope  
470 analysis with the denitrifier method, *Rapid Commun Mass Spectrom*, 23, 3753-3762, 2009.
- 471 Grasshoff, K., Kremling, K., and Ehrhardt, M.: *Methods of Seawater Analysis*, Wiley-VCH, Weinheim,  
472 1999.
- 473 Hartmann, M., Müller, P., Suess, E., and Van der Weijden, C. H.: Oxidation of organic matter in recent  
474 marine sediments, *Meteor Forschungs-Ergebnisse, Reihe C*, 74-86, 1973.

475 Heip, C. H. R., Goosen, N. K., Herman, P. M. J., Kromkamp, J., Middelburg, J. J., and Soetaert, K.:  
476 Production and consumption of biological particles in temperate tidal estuaries, *Oceanography and*  
477 *Marine Biology*, 33, 1-149, 1995.

478 Hellemann, D., Tallberg, P. and Hietanen, S.: Benthic N<sub>2</sub> production rates, Si cycling and  
479 environmental characteristics from the Öre estuary on the Swedish coast, *Marine Ecology Progress*  
480 *Series*, 583, 63-80, 2017.

481 Henriksen, K. and Kemp, W. M.: Nitrification in Estuarine and Coastal Marine Sediments. In: *Nitrogen*  
482 *Cycling in Coastal Marine Environments*, Blackburn, T. H. and Sorensen, J. (Eds.), John Wiley & Sons  
483 Ltd, SCOPE, 1988.

484 Hickel, W., Mangelsdorf, P., and Berg, J.: The human impact in the German Bight: Eutrophication  
485 during three decades (1962-1991), *Helgoländer Meeresun*, 47, 243-263, 1993.

486 Hydes, D. J., Kelly-Gerreyn, B. A., Le Gall, A. C., and Proctor, R.: The balance of supply of nutrients and  
487 demands of biological production and denitrification in a temperate latitude shelf sea – a treatment  
488 of the southern North Sea as an extended estuary, *Marine Chemistry*, 68, 117-131, 1999.

489 Jensen, K. M., Jensen, M. H., and Kristensen, E.: Nitrification and denitrification in Wadden Sea  
490 sediments (Konigshafen, Island of Sylt, Germany) as measured by nitrogen isotope pairing and  
491 isotope dilution, 11, 181-191, 1996.

492 Jorgensen, B. B.: Mineralization of organic matter in the sea bed-the role of sulphate reduction,  
493 *Nature*, 296, 643-645, 1982.

494 Jorgensen, B. B.: Processes at the sediment-water interface. In: *The Major Biogeochemical Cycles and*  
495 *Their Interactions*, Bolin, B. and Cook, R. B. (Eds.), John Wiley, New York, 1983.

496 Kana, T. M., Darkangelo, C., Hunt, M. D., Oldham, J. B., Bennett, G. E., and Cornwell, J. C.: Membrane  
497 Inlet Mass Spectrometer for Rapid High-Precision Determination of N<sub>2</sub>, O<sub>2</sub>, and Ar in Environmental  
498 Water Samples.pdf>, *Analytical Chemistry*, 66, 4166-4170, 1994.

499 Kérouel, R. and Aminot, A.: Fluorimetric determination of ammonia in sea and estuarine water by  
500 direct segmented flow analysis. , *Marine Chemistry*, 57, 265-275, 1997.

501 Koike, I. and Hattori, A.: Simultaneous determinations of nitrification and nitrate reduction in coastal  
502 sediments by a <sup>15</sup>N dilution technique, *Appl Environ Microbiol*, 35, 853-857, 1978.

503 Krämer, K., Holler, P., Herbst, G., Bratek, A., Ahmerkamp, S., Neumann, A., Bartholoma, A., van  
504 Beusekom, J. E. E., Holtappels, M., and Winter, C.: Abrupt emergence of a large pockmark field in the  
505 German Bight, southeastern North Sea, *Sci Rep*, 7, 5150, 2017.

506 Lenhart, H. J. and Pohlmann, T.: The ICES-boxes approach in relation to results of a North Sea  
507 circulation model, *Tellus A: Dynamic Meteorology and Oceanography*, 49, 139-160, 1997.

508 Lohse, L., Malschaert, J. F. P., Slomp, C. P., Helder, W., and van Raaphorst, W.: Nitrogen cycling in the  
509 North Sea sediments: interaction of denitrification and nitrification of offshore and coastal areas,  
510 *Marine Ecology Progress Series*, 101, 283-296, 1993.

511 LOICZ: Land-Ocean Interactions in the Coastal Zone, 1995.

512 Los, F. J., Troost, T. A., and Van Beek, J. K. L.: Finding the optimal reduction to meet all targets—  
513 Applying Linear Programming with a nutrient tracer model of the North Sea, *Journal of Marine*  
514 *Systems*, 131, 91-101, 2014.

515 Marchant, H. K., Holtappels, M., Lavik, G., Ahmerkamp, S., Winter, C., and Kuypers, M. M. M.:  
516 Coupled nitrification-denitrification leads to extensive N loss in subtidal permeable sediments,  
517 *Limnology and Oceanography*, 61, 1033-1048, 2016.

518 Neubacher, E. C., Parker, R. E., and Trimmer, M.: Short-term hypoxia alters the balance of the  
519 nitrogen cycle in coastal sediments, *Limnology and Oceanography*, 56, 651-665, 2011.

520 Neumann, A.: Elimination of reactive nitrogen in continental shelf sediments measured by  
521 membrane inlet mass spectrometry., PhD, Department Geowissenschaften, Universität Hamburg,  
522 Hamburg, 2012.

523 Neumann, A., van Beusekom, J. E. E., Eisele, A., Emeis, K.-C., Friedrich, J., Kröncke, I., Logemann, E. L.,  
524 Meyer, J., Naderipour, C., Schückel, U., Wrede, A., and Zettler, M.: Elucidating the impact of  
525 macrozoobenthos on the seasonal and spatial variability of benthic fluxes of nutrients and oxygen in  
526 the southern North Sea, in preparation. in preparation.



527 Neumann A., Möbius J., Hass H. C., Puls W., Friedrich J.: Empirical model to estimate permeability of  
528 surface sediment in the German Bight (North Sea). *Journal of Sea Research* 127, 36-45, 2016.

529 Neumann, A., van Beusekom, J. E. E., Holtappels, M., and Emeis, K.-C.: Nitrate consumption in  
530 sediments of the German Bight (North Sea), *Journal of Sea Research*, 127, 26-35, 2017.

531 Nishio, T., Komada, M., Arao, T., and Kanamori, T.: Simultaneous determination of transformation  
532 rates of nitrate in soil, *Japan Agricultural Research Quarterly: JARQ*, 35, 11-17, 2001.

533 OSPAR: Quality Status Report, London, 176 pp pp., 2010.

534 Pätsch, J. and Lenhart, H.-J.: Daily loads of nutrients, total alkalinity, dissolved inorganic carbon and  
535 dissolved organic carbon of the European continental rivers for the years 1977-2002. In: *Berichte aus  
536 dem Zentrum für Meeres- und Klimaforschung, Reihe B: Ozeanographie*, University of Hamburg,  
537 Germany, 2004.

538 Redfield, A. C.: The biological control of chemical factors in the environment, *American Scientist*, 46,  
539 205-221, 1958.

540 Rysgaard, S., Risgaard-Petersen, N., and Sloth, N. P.: Nitrification, denitrification and nitrate  
541 ammonification in two coastal lagoons in Southern France, *Hydrobiologia*, 329, 133-141, 1996.

542 Sanders, T., Schöl, A., and Dähnke, K.: Hot spots of nitrification in the Elbe Estuary and their impact  
543 on nitrate regeneration, *Estuaries and Coasts*, 41, 128-138, 2018.

544 Seitzinger, S. P. and Giblin, A. E.: Estimating denitrification in North Atlantic continental shelf  
545 sediments, *Biogeochemistry*, 35, 235-260, 1996.

546 Sigman, D. M., Casciotti, K. L., Andreani, M., Barford, C., Galanter, M., and Böhlke, J. K.: A bacterial  
547 method for the nitrogen isotopic analysis of nitrate in seawater and freshwater, *Anal. Chem.*, 73,  
548 4145-4153, 2001.

549 Thibodeau, B., Lehmann, M. F., Kowarzyk, J., Mucci, A., Gélinas, Y., Gilbert, D., Maranger, R., and  
550 Alkhatib, M.: Benthic nutrient fluxes along the Laurentian Channel: Impacts on the N budget of the  
551 St. Lawrence marine system, *Estuarine, Coastal and Shelf Science*, 90, 195-205, 2010.

552 Van Beusekom, J., Brockmann, U. H., Hesse, K.-J., Hickel, W., Poremba, K., and Tillmann, U.: The  
553 importance of sediments in the transformation and turnover of nutrients and organic matter in the  
554 Wadden Sea and German Bight, *German Journal of Hydrography*, 51, 245-266, 1999.

555 van Leeuwen, S. M., van der Molen, J., Ruardij, P., Fernand, L., and Jickells, T.: Modelling the  
556 contribution of deep chlorophyll maxima to annual primary production in the North Sea,  
557 *Biogeochemistry*, 113, 137-152, 2013.

558 von Westernhagen, H., Hickel, W., Bauerfeind, E., Niermann, U., and Kröncke, I.: Sources and effects  
559 of oxygen deficiencies in the south-eastern North Sea, *Ophelia*, 26, 457-473, 1986.

560 Zhang, L., Altabet, M. A., Wu, T., and Hadas, O.: Sensitive Measurement of  $\text{NH}_4^+ \text{ }^{15}\text{N}/^{14}\text{N}$  ( $\delta^{15}\text{NH}_4^+$ ) at  
561 Natural Abundances Levels in Fresh and Saltwaters, *Anal Chem*, 79, 5297-5303, 2007.

562 **Table 1: Rates of nitrification, dissimilatory nitrogen reduction to ammonia (DNRA), anaerobic ammonia oxidation**  
563 **(anammox) and denitrification (DNIT) (in  $\mu\text{mol N m}^{-2} \text{d}^{-1}$ ) in the North Sea of other published data. Abbreviation of**  
564 **methods: SIDM - sediment isotope dilution method; MABT - modified acetylene block technique; SSI - sediment slurry**  
565 **incubations, PWMI – pore-water mean fitting, IPT - isotope-pairing technique.**

Location	Nitrification	DNRA	Anammox	DNIT rate / NO <sub>3</sub> <sup>-</sup> uptake	Sediment type	C <sub>org</sub>	C:N	Sampling time	Method	Reference	
											[ $\mu\text{mol m}^{-2} \text{d}^{-1}$ ]
German Bight (North Sea)	1233 ± 12	N.D.	N.D.	1314 ± 1087	medium sand	0.03	<0.01	08./09.2016	SIDM	this study	
	1739 ± 695	N.D.	N.D.	1355 ± 876	Fine sand	0.04	0.01				
	1271	N.D.	N.D.	1306 ± 1042		0.21	0.03				
	2069 ± 63	N.D.	N.D.	1915 ± 831	clay/silt	0.73	0.10				
Dutch Coast	N.D.	N.D.	N.D.	N.D.	fine sand	0.03	N.D.	11.2010	SSI	(Bale et al., 2014)	
								02.2011			
								05.2011			
								08.2011			
Oyster Ground	N.D.	N.D.	N.D.	N.D.	muddy sand / clay / silt	0.30	N.D.	11.2010	SSI	(Bale et al., 2014)	
								02.2011			
								05.2011			
								08.2011			
North Dogger	N.D.	N.D.	N.D.	N.D.	fine sand	0.03	N.D.	11.2010	SSI	(Bale et al., 2014)	
								02.2011			
								05.2011			
								08.2011			
Elbe Estuary / coastal zones	N.D.	N.D.	N.D.	771*	coarse sand	0.6	6.0	03.2009	IPT	(Deek et al., 2013)	
				1215*		0.1	N.D.				
				3200*		0.1	N.D.				
				864*		0.6	6.0				
				1425*		0.2	N.D.	09.2009			
				47*		0.1					
				140*		0.2					
				12.0*		0.12					6.0
Oyster Ground	288 ± 144	N.D.	N.D.	19.2*	muddy sand	0.16	8.0	08.1991	MABT	(Lohse et al., 1993)	
	192 ± 96			02.1992							
Weiss Bank	216	N.D.	N.D.	21.6*	muddy sand	0.16	5.3	08.1991	MABT	(Lohse et al., 1993)	
	120 ± 120			02.1992							
Tail End	432 ± 168	N.D.	N.D.	2.4*	fine sand	0.06	6.0	08.1991	MABT	(Lohse et al., 1993)	
	264 ± 120			02.1992							
Esbjiberg	408 ± 216	N.D.	N.D.	9.6*	fine sand	0.06	6.0	08.1991	MABT	(Lohse et al., 1993)	
	168 ± 168			02.1992							
Helgoland	0	N.D.	N.D.	91.2*	silt	1.28	8.5	08.1991	MABT	(Lohse et al., 1993)	
	216 ± 1220			02.1992							
Elbe Rinne	264 ± 72	N.D.	N.D.	4.8*	muddy sand	0.46	9.2	08.1991	MABT	(Lohse et al., 1993)	
	288 ± 96			02.1992							
Frison Front	624 ± 288	N.D.	N.D.	16.8*	muddy sand	0.46	9.2	08.1991	MABT	(Lohse et al., 1993)	
	192 ± 72			02.1992							
Sylt	81.6 ± 64.8	N.D.	N.D.	372 ± 132*	coarse sand	N.D.	N.D.	06.1993	IPT, SIDM	(Jensen et al., 1996)	
	11 ± 2			44.5 ± 13.5*				04.1994			
	3.8 ± 1.6			17 ± 4*				04.1994			
	1116 ± 924			75 ± 39*				03.1993			
Helgoland	1150 ± 700	N.D.	N.D.	103.5 ± 17.5*	muddy sand	N.D.	N.D.	04.1994	IPT, SIDM	(Jensen et al., 1996)	
	210 ± 50			870 ± 100*				03.1993			
	2980 ± 420			2280 ± 300*				04.1994			
Sean Gras	N.D.	N.D.	N.D.	24.0	medium sand	0.05	8.1	04.2007	IPT	(Neubacher et al., 2011)	
				24.0				72*			05.2007
				0				120*			09.2007
				48.0				144*			10.2007
				0				24*			N.D.
				24				288*			10.2
				24				120*			02.2007
				24				120*			02.2007
				120				408*			09.2007
				144				504*			10.2007
				48				144*			04.2008
				0				24*			10.2
North Dogger	N.D.	N.D.	N.D.	24	muddy sand	0.45	9.4	04.2007	IPT	(Neubacher et al., 2011)	
				0				96*			04.2007
				24				168*			05.2007
				48				288*			09.2007
German Bight / Dogger Bank	N.D.	N.D.	N.D.	20.5 ± 4.5**	mud	0.37 ± 0.02	N.D.	05.2009	PWMI	(Neumann et al., 2017)	
				28.5 ± 23.5**				0.16 ± 0.12			02.2010
				8 ± 8**				0.13 ± 0.10			05.2009
				12.5 ± 12.5**				0.10 ± 0.08			02.2010
				59.5 ± 25.5**				0.16 ± 0.13			05.2009
				99 ± 35.0**				0.02			02.2010

566 N.D. – not determined

567 \* Denitrification

568 \*\* NO<sub>3</sub><sup>-</sup> uptake

**Table 2: Characteristics of bottom water and sediment characteristics of the sampled stations in the North Sea (<https://doi.org/10.1594/PANGAEA.846041>). C<sub>org</sub> means organic carbon content and TN means total nitrogen content of the surface sediment.**

Location	Depth	Sediment core	Incubation time	Sediment type	C <sub>org</sub>	TN	Porosity	Permeability	Temp.	Salinity	OPD
[-]	[m]	[-]	[hours]	[-]	[%]	[%]	[-]	[m <sup>2</sup> ]	[°C]	[-]	[mm]
NOAH-A	31.0	1	24	medium sand	0.03*	≤0.01*	0.37	1.7*10 <sup>-10</sup>	19.1	33.7	>15
		2	24								
		3	18								
		4	24								
NOAH-C	25.4	1	24	clay/silt	0.73	0.10	0.56	1*10 <sup>-15</sup>	19.1	32.5	3.6
		2	24								
		3	24								
NOAH-D	38.0	1	18	fine sand	0.21	0.03	0.43	1.4*10 <sup>-13</sup>	18.9	33.0	2.4
		2	24								
		3	24								
NOAH-E	28.4	1	18	medium sand	0.04	0.01	0.41	8.8*10 <sup>-12</sup>	18.7	32.4	4.2
		2	18								
		3	24								
		4	24								

\* estimated

**Table 3: Rates of benthic net NO<sub>3</sub><sup>-</sup> and benthic net NH<sub>4</sub><sup>+</sup> fluxes per area, water depth below thermocline (average value of all sediment cores per station) and concentration of dissolved inorganic nitrogen (DIN) in the thermocline. Bottom water concentration of nitrate (cNO<sub>3</sub><sup>-</sup>), nitrite (cNO<sub>2</sub><sup>-</sup>) and ammonium (cNH<sub>4</sub><sup>+</sup>). The concentration of DIN per area was calculated by the multiplication of the water depth below the thermocline with the concentration of DIN. Turnover rates of nitrogen were calculated by the division of DIN per area with the rates of NH<sub>4</sub><sup>+</sup><sub>net</sub> and NO<sub>3</sub><sup>-</sup><sub>net</sub> and the effect of sedimentary N release on the reactive nitrogen available for primary production in the water column.**

Station	rNH <sub>4</sub> <sup>+</sup> <sub>net</sub> + rNO <sub>3</sub> <sup>-</sup> <sub>net</sub>	Water depth below thermocline	cNO <sub>3</sub> <sup>-</sup>	cNO <sub>2</sub> <sup>-</sup>	cNH <sub>4</sub> <sup>+</sup>	DIN per area	N turnover	sedimentary N support for primary production
[-]	[mmol m <sup>-2</sup> d <sup>-1</sup> ]	[m]	[μmol L <sup>-1</sup> ]			[mmol m <sup>-2</sup> ]	[days]	[%]
NOAH-A	1.6 ± 0.4	29.5	0.1	< 0.1	0.6 ± 0.2	20.7	10.8 ± 0.3	14.1 ± 4.7
NOAH-C	6.6 ± 1.4	10.0	< 0.1	0.7	2.0 ± 0.2	30.0	3.4 ± 0.1	58.7 ± 10.6
NOAH-D	0.5 ± 0.1	38.0	0.1 ± 0.1	0.1	0.8 ± 0.6	26.6	28.5 ± 0.6	7.1 ± 2.6
NOAH-E	3.2 ± 0.6	10.0	< 0.1	< 0.1	0.3 ± 0.1	3.0	0.9 ± 0.1	26.5 ± 14.3

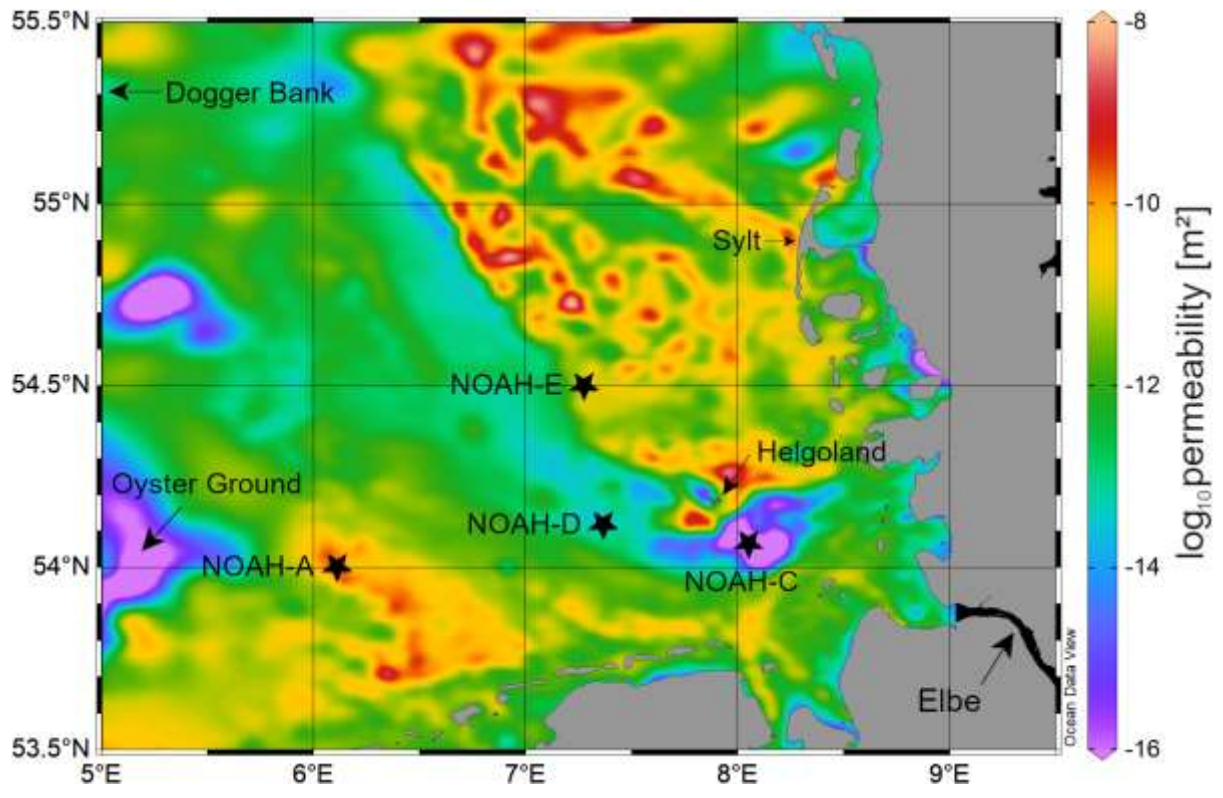


Figure 1: Map showing the sampling stations NOAH-A, NOAH-C, NOAH-D and NOAH-E in the German Bight in the North Sea. Colored areas show the spatial variability of surface sediment permeability (<https://doi.org/10.1594/PANGAEA.872712>).

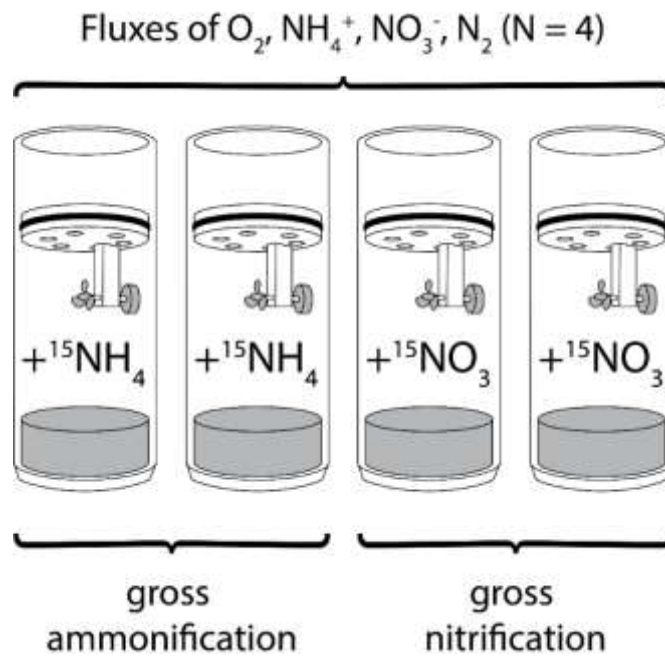


Figure 2: Schematic illustration of the experimental setup. Four sediment cores were incubated to measure benthic fluxes of oxygen, ammonium, nitrate, and  $N_2$ . Two of these flux cores were amended with either  $^{15}NH_4^+$  or  $^{15}NO_3^-$  for the measurement of gross rates of ammonification and nitrification, respectively.

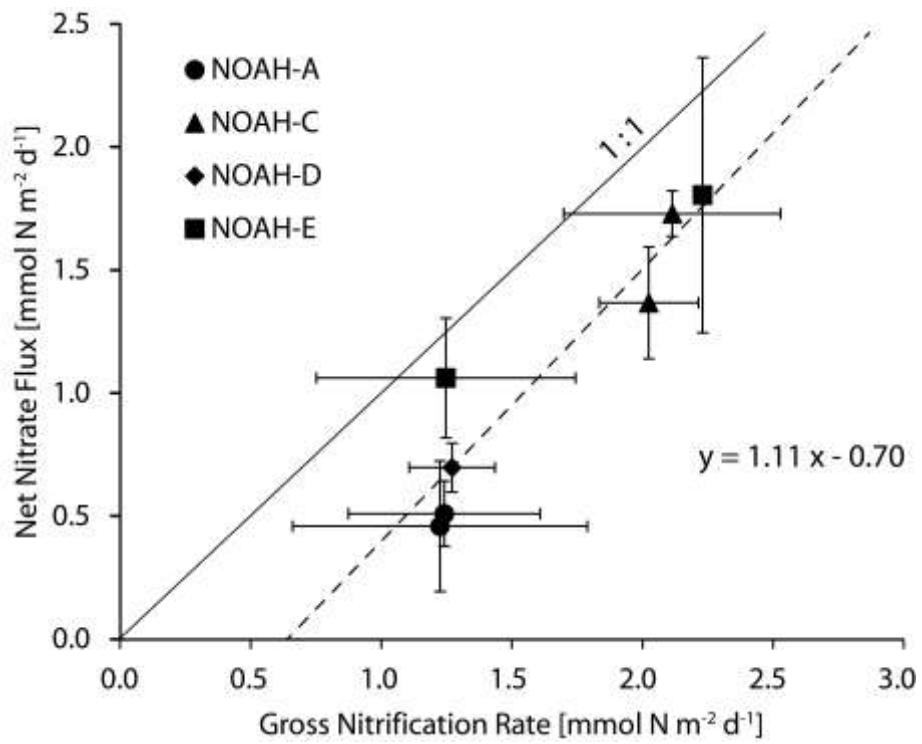


Figure 3: Correlation of gross nitrification rates and actual nitrate fluxes. The solid line indicates the 1:1 ratio, the dashed line indicates the linear regression. The error bars indicate the regression error of individual rates at the 0.95 confidence level.

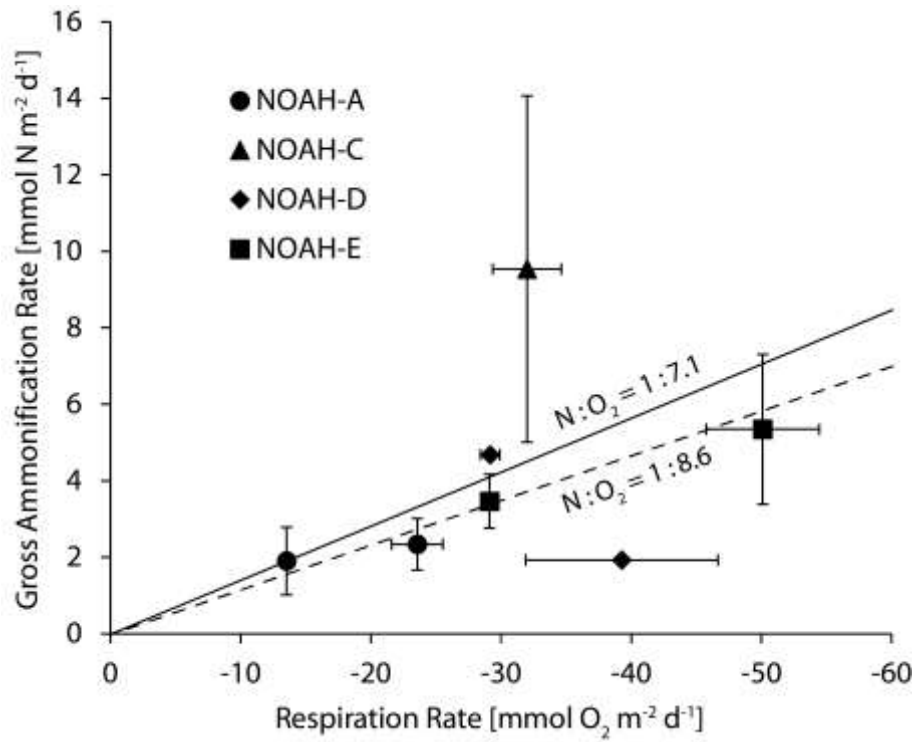


Figure 4: Benthic O<sub>2</sub> fluxes and gross ammonification rates of the sampled stations. The dashed line indicates the Redfield ratio of oxygen and nitrogen (N:O<sub>2</sub> 1:8.625) (Redfield, 1958), and the solid lines indicates the ratio of oxygen and nitrogen determined by the C/N ratio in the North Sea (N:O<sub>2</sub> 1:7.1). The error bars indicate the regression error of individual rates at the 0.95 confidence level.

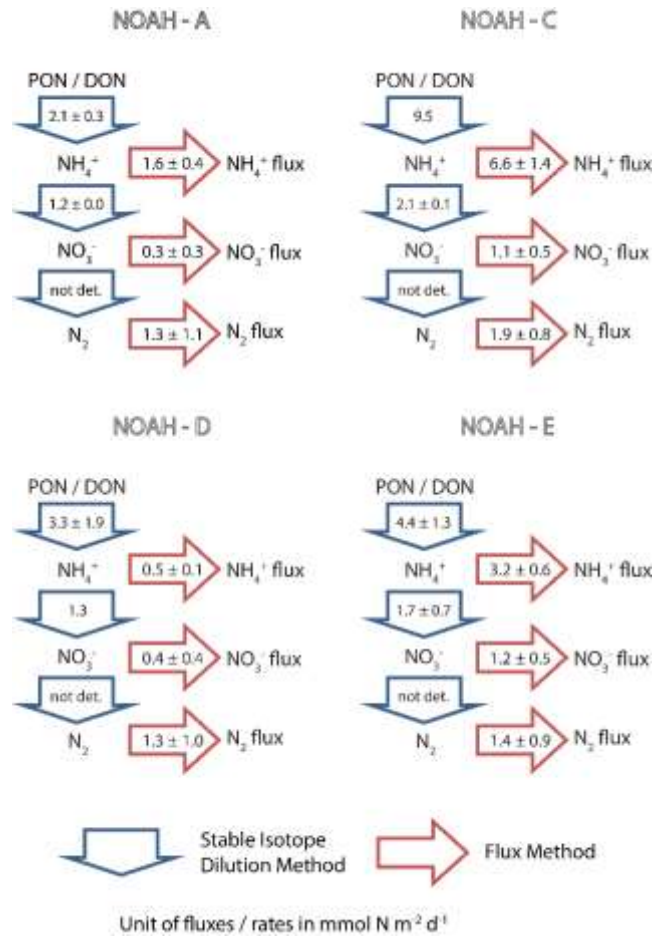


Figure 5: Benthic N-transformation rates (in mmol N m<sup>-2</sup> d<sup>-1</sup>) of ammonification ( $\text{NH}_4^+$ ) and nitrification ( $\text{NO}_3^-$ ) as measured by means of stable isotope methods (blue arrows). Simultaneously measured fluxes of ammonium ( $\text{NH}_4^+$  flux), nitrate ( $\text{NO}_3^-$  flux), and  $\text{N}_2$  (in mmol N m<sup>-2</sup> d<sup>-1</sup>) as measured by the flux method (red arrows).